Evidence of dengue virus transmission and a diverse *Aedes* mosquito virome on the Democratic Republic of Congo-Angola border

Running title: *Aedes* mosquito virome in the DRC

Wenqiao He[1#], Thierry Bobanga[2], Anne Piantadosi[3,4], Zachary R. Popkin-Hall[1], Fabien Vulu[2], Matthew H. Collins[4], Melchior M. Kashamuka[5], Antoinette K. Tshefu[5], Jonathan J. Juliano[1*], Jonathan B. Parr[1*#]

[1] Institute for Global Health and Infectious Diseases and Division of Infectious Diseases, Department of Medicine, University of North Carolina at Chapel Hill, Chapel Hill, NC, United States

[2] Department of Tropical Medicine, Faculty of Medicine, University of Kinshasa, Kinshasa, Democratic Republic of the Congo

[3] Department of Pathology and Laboratory Medicine, Emory University School of Medicine, Atlanta, GA, USA

[4] Division of Infectious Diseases, Department of Medicine, Emory University School of Medicine, Atlanta, GA, USA

[5] Kinshasa School of Public Health, Kinshasa, Democratic Republic of the Congo

* Co-senior authors

[#] Corresponding authors: wenqiao@email.unc.edu; jonathan_parr@med.unc.edu

Abstract

Aedes mosquitoes are widely distributed across the Democratic Republic of Congo (DRC), and are major vectors of dengue (DENV), Zika, chikungunya (CHIKV), and yellow fever (YFV) viruses. While the high burden of malaria in the DRC receives considerable attention, arboviruses remain understudied. In the setting of recent CHIKV and YFV outbreaks in southwestern DRC, we collected *Aedes* mosquitoes in three areas of Kimpese, DRC, near the Angola border, to investigate their virome. Metagenomic and targeted sequencing of eight randomly selected field mosquito pools, comprising 155 mosquitoes from three collection sites, confirmed high-confidence DENV reads and human blood meals in six (75%) and eight (100%) pools, respectively. We find diverse mosquito viromes including other known and putative human and animal viruses. Our findings provide strong evidence of endemic DENV transmission along the DRC-Angola border and illustrate the potential of wild-caught mosquitoes for xenosurveillance of emerging pathogens.

Keywords: *Aedes* mosquito, dengue, Democratic Republic of Congo, viral metagenomic

Introduction

Arthropod-borne pathogens, including viruses, bacteria, and parasites, account for more than 17% of all infectious diseases [1,2], and over 700 arboviruses have been documented to infect humans across a wide geographic distribution [3,4]. The number of outbreaks and endemic infections caused by emergent and re-emergent mosquito-borne arboviruses have increased worldwide over the last two decades [5–7]. *Aedes* mosquitoes are particularly important vectors for multiple important human pathogens, including dengue virus (DENV), Zika virus (ZIKV), yellow fever virus (YFV), and chikungunya virus (CHIKV) [8–11]. The warm climate and suitable environmental conditions in tropical regions support the proliferation of both mosquitoes and the viruses they transmit. As a result, tropical regions tend to have higher diversity and prevalence of arboviruses than other regions. However, arbovirus transmission is understudied across Africa, where improved understanding is urgently needed to guide roll out of newly available DENV vaccines, in particular [12].

The Democratic Republic of the Congo (DRC) is the largest country in central Africa with a population of over 100 million, and a tropical climate conducive to mosquitoes. Approximately 248 mosquito species are thought to reside in the DRC [13], including *Aedes aegypti* and *Aedes albopictus*, both of which are major disease vectors [7,14]. A recent survey found that *Ae. albopictus* is expanding its distribution in the DRC and displacing native *Aedes* species [15]. Chikungunya, YFV, and DENV outbreaks and infections are known to occur in the DRC [16–18], and increasing reports of mosquito-borne and emerging viral diseases have been recorded [19]. Considerable attention is devoted to the high burden of malaria [20] in the DRC, but arboviruses remain neglected, with limited studies of humans and mosquitoes to-date [3,17–19,21]. The lack of diagnostic tools and surveillance systems for these diseases hinders our understanding of their impact and epidemiology [22].

Metagenomic sequencing approaches can be used for identification of viral DNA and/or RNA within diverse sample types. These methods have recently been applied to mosquito virome analyses, particularly in the context of mosquito-borne pathogen transmission and xenosurveillance, to enhance understanding of host–vector–environment interactions and support integrated monitoring of pathogens and exposures at the interface of animal and public health [23–26]. To improve our understanding of the role of *Aedes* mosquito vectors in arboviral transmission in the DRC, we collect and sequence the virome of mosquito pools from three areas of Kimpese, a region near the Angola border which has experienced recent arboviral outbreaks (**Figure 1**). We observe diverse viromes and identify strong evidence of

active DENV transmission in the region, corroborated by viral sequences, DENV PCR, and mosquito blood meal analysis.

Results

Mosquito collection and species confirmation

More than 600 adult *Aedes* mosquitoes **(Table S1)** were collected and distributed into 37 pools based on sample collection sites (21 pools from Kimpese city, 6 pools from Malanga, and 10 pools from Viaza, **Figure 2a**). Three species of *Aedes* mosquitoes were identified by morphology: *Aedes albopictus (n=653, 98.34%)*, *Aedes aegypti (n=8, 1.20%)*, and *Aedes simpsoni (n=3, 0.45%)*. Among the eight sequenced pools (**Figure 2b**), all contained majority *Ae. albopictus* (**Table S2**) based on their *ITS2* and *COI* gene sequences.

Sequencing output

A total of 3,795,246,904 raw reads were obtained by Illumina sequencing. A range of 78.2-84.4% paired-end reads in each field mosquito pool were successfully merged. After filtering out low quality reads and those mapping to host and contaminating contigs (**Figure 3a and Table S3**), 185,621,738 reads remained, of which 144,469,836 were unclassified reads (77.8% of total) that did not map to any sequences in the KrakenUniq default nt database. Classified reads were mapped to known viruses, bacteria, eukaryota, and archaea.

Viral metagenomic analysis

Results confirm a highly diverse virome in wild-caught *Aedes* from the DRC, with viruses specific to invertebrates, vertebrates, plants, bacteria, fungi, and protozoa, as well as an unclassified group of viruses (**Figure 3b**). We do not observe a correlation between the number of viral taxa and the number of mosquitoes in the field-collected mosquito pools.

Most of the viral genera detected in the laboratory-uninfected *Ae. aegypti* mosquito pool and the water control are not found in the field mosquito pools (**Table S4**). Although reads annotated as viral genera *Betacoronavirus*, *Mimivirus*, and *Pahexavirus* are detected in both the water control and some field mosquito pools, BLAST results show no true matches to *Betacoronavirus* in the water control and reveal that the *Mimivirus* and *Pahexavirus* reads in field mosquito pools mapped to different genomic regions than those in the water control; therefore, no reads in field mosquito pools are removed in this filtering step. Based on taxonomic classification using the KrakenUniq with the NCBI-nt database, and after applying the RPM < 10 threshold and index-hopping filter, we identify 33 unique total viral families

and 28 unique total viral genera in the field mosquito pools, with each pool containing between 3-17 viral families and 2-16 viral genera (**Figure 4, S1, and S2, Supplementary Material**).

Flaviviridae is found in all field mosquito pools collected from Kimpese city and Viaza. *Orthoflavivirus,* which includes viruses formerly classified under the *Orthoflavivirus* and *Flavivirus* genera [27], is the most abundant viral genus in most Kimpese mosquito pools (except K2) and all Viaza pools, with a large number of reads mapping to *Orthoflavivirus denguei*. K2 contains a large number of reads annotated as genus *Cripavirus* (family *Dicistroviridae*). *Jonvirus*, a genus typically associated with insect viruses, shows the highest relative abundance in the mosquito pool from Malanga and is exclusively detected in that pool.

Several viral genera capable of infecting humans and animals are detected in mosquito pools collected from Kimpese city. These include *Betacoronavirus* (family *Coronaviridae*), *Marseillevirus* (family *Marseilleviridae*), and *Simplexvirus* (family *Herpesviridae*). Genus *Orthophasmavirus* is found exclusively in Kimpese pools, while *Alphabaculovirus* and *Alphamesonivirus* are detected only in the mosquito pool from Malanga. These genera contain insect-associated viruses. *Muromegalovirus*, a genus within the family *Herpesviridae* known to naturally infect rodents, is detected exclusively in one Viaza pool and is not in mosquito pools from Kimpese city and Malanga. All corresponding reads map to viral species *Muromegalovirus muridbeta2*.

PCA based on detected viral genera to explore clustering by sample collection area is shown in **Figure S3 and Table S5**. Geographical clustering is observed among samples from Kimpese city and Viaza. Notably, two mosquito pools from Kimpese city differ substantially from the other three pools collected at the same site.

KrakenUniq annotation results prior to applying the RPM < 10 threshold and index-hopping filter are provided in the Supplementary Notes. These datasets include all viral sequences remaining after initial quality filtering steps, such as removal of low-quality reads, host-derived sequences, and contaminant contigs or reads, providing a comprehensive overview of the detected viral diversity. Notably, some pathogens and potential pathogens were detected with low read counts, including *human pegivirus* and *human blood-associated dicistrovirus*.

Insect-specific viruses

136 We find a large number of insect-specific viruses in field mosquito pools, with most
137 belonging to the families *Solemoviridae* and *Flaviviridae*. *Wenzhou sobemo-like virus 4*,
138 *Hubei mosquito virus 2*, *Guangzhou sobemo-like virus*, *Sichuan mosquito sobemo-like virus*,
139 and *Aedes flavivirus* are the most prevalent species (**Table S6**). Except for *Wenzhou*
140 *sobemo-like virus 4* (6/8, 75%), the other four insect-specific viruses are detected in 7 out of
141 8 (87.5%) mosquito pools with high relative abundance.

142 **Phylogenetic analysis of reads mapping to pathogens and potential pathogens**

143 BLAST-confirmed reads mapping to viral species related to human or animal diseases are
144 detected in multiple mosquito pools, including DENV and *bat faecal associated dicistrovirus*
145 *4* (**Figure 5a**). Though SPAdes does not successfully assemble any contigs spanning
146 multiple DENV reads in this study, BLAST-confirmed, merged paired-end reads mapping to
147 DENV are found in 6 out of the 8 (75%) field mosquito pools (**Table S7**). Reads mapping to
148 DENV-2 in one mosquito pool (K5) are highly similar to one sequence from Malaysia
149 (MH048672.1 10664-10770, 107 bp, nucleotide identity = 94%, **Figure 5b and 6a**). Reads
150 mapping to DENV-4 found in all six positive pools are short (< 100bp) and show high
151 similarity to the 5'-untranslated (UTR) region of a published sequence from Thailand
152 (MG601754.1 1-90, nucleotide identity = 97.8%) (**Figure 5b and 6b**). Amplification of
153 polyprotein genes and other fragments using published assays failed [28–30], likely due to low
154 DENV RNA concentration and RNA degradation within mosquito pools (median peak RNA
155 fragment length 176 nt, IQR 115-178). We note that these DENV-4 reads also map to
156 Wenzhou sobemo-like virus 4 sequences, but with lower similarity (nucleotide identity ≤
157 96.67%) and higher e-values. Phylogenetic analysis of these short, merged paired-end
158 reads suggests the presence of DENV types 2 and 4 in the DRC, though resolution is
159 limited.

160 We find high similarity between reads mapping to *bat fecal-associated dicistrovirus 4* to a
161 published *bat faecal associated dicistrovirus 4* sequence detected in feces from *Pteropus*
162 *poliocephalus* from Australia (ON872534.1, 7078-7330, 253 bp) in three mosquito pools
163 (**Figure 5a**). However, we are unable to assemble contigs for this virus, and resolution of
164 phylogenetic analysis is limited. Additional details on these viral reads are provided in **Figure**
165 **7** and **Table S8**.

166 **PCR confirmation of DENV and mosquito blood meal investigation**

167 Real-time PCR targeting the DENV polyprotein gene, distinct from genomic regions included
168 in our phylogenetic analysis, confirms DENV RNA in the three mosquito pools with highest

169 DENV read counts in metagenomic analysis (**Table S7**), indicating consistency between
170 next-generation sequencing and real-time PCR within its limits of detection.

171 Investigation of mosquito blood meals using amplicon sequencing showed that mosquitoes
172 from all selected pools had taken blood from *Homo sapiens* (**Figure 8**). Additionally, we
173 detect reads mapping to non-human primates (4/8 pools), rodents (3/8 pools), canines (3/8
174 pools), and sheep (1/8 pools).

175 Discussion

176 Our findings confirm the presence of dengue and other viruses with human or animal
177 pathogenic potential in wild-caught *Aedes* mosquitoes circulating near the DRC's border with
178 Angola. The presence of human blood in all mosquito pools suggests active dengue
179 transmission in the Kimpese region, including peri-urban and rural zones outside of the city.
180 The combination of a diverse mosquito virome and the presence of blood meals from
181 multiple mammals suggests robust opportunities for arthropod-borne viral transmission
182 between species, as well as for spillover events. Together, our experience suggests a future
183 role for xenosurveillance and metagenomic sequencing as a complement to existing data
184 systems developed to monitor for emerging infectious diseases in countries like the DRC.

185 Multiple arboviral disease outbreaks have been documented in the DRC during the last
186 century, including yellow fever, dengue, chikungunya, and others [3,17,18,21]. Except for DENV,
187 we did not find other known human pathogenic arboviruses in the selected *Aedes* pools.
188 Detection of DENV in mosquito pools by RT-PCR suggests active DENV circulation in the
189 Kimpese region, and metagenomic sequencing reads from small regions of the genome
190 point towards the circulation of both DENV-2 and DENV-4. Three of the four DENV
191 serotypes [31] have been recorded in the human population of the DRC (DENV-1, DENV-2,
192 and DENV-3), with DENV-1 being the most frequently reported [3]. One study in Singapore
193 reported that the majority of the dengue hemorrhagic fever cases involving DENV-2 were
194 from the cosmopolitan genotype [32]. DENV-2 detected in our study is most similar to the
195 cosmopolitan genotype of DENV-2, which has been previously reported in the DRC [33]. The
196 DENV-2 reads detected in our study show closer similarity to cosmopolitan DENV-2 from
197 Malaysia than to DENV-2 sequences previously reported from the DRC, however this
198 comparison is based on small genome fragments. Although the DENV-4 reads detected in
199 our study also map to Wenzhou sobemo-like virus 4, an insect-specific virus, they have
200 lower similarity (nucleotide identity ≤96.67%) and higher e-values. Our study provides
201 preliminary evidence that DENV-4 may circulate in *Aedes* mosquitoes from the DRC and
202 therefore infect people in this region.

203 Data from all *Aedes* mosquito pools in our study confirm human blood meals. Previous
204 studies have reported high dietary diversity of *Aedes* mosquitoes, with a predominant
205 preference for mammalian hosts [34,35]. We corroborate these findings, with diverse
206 mammalian blood meals observed across mosquito pools, including blood from non-human
207 primates. Non-human primates can be amplifying hosts and play considerable roles in the
208 sylvatic cycle of DENV transmission, which can spark DENV epidemics in nearby human
209 populations [36]. Detection of rodent, canine, and sheep genomes in the collected mosquito
210 pools illustrate the diversity of hosts of *Aedes*, though further research is needed to confirm
211 the roles of these hosts in DENV transmission, including the contribution to human infection.
212 Notably, three (K2, K4, and V3) mosquito pools appear to have exclusively fed on human
213 blood.

214 Similar windows of detection have been observed for pathogen RNA and human DNA in
215 mosquitoes following a blood meal. Past work has shown complete digestion of a human
216 blood meal varies depending on the mosquito species and typically takes about 36 hours to
217 3 days [37,38]. The persistence of pathogen RNA or DNA in mosquitoes can vary depending on
218 the pathogen type, viral strain, viral load, and mosquito species. Non-arboviral RNA can
219 remain detectable in the mosquito midgut for a field-relevant time-frame—up to 18 hours for
220 west nile virus RNA and up to 24 hours for HIV-1 RNA after blood feeding [39]. Influenza virus
221 RNA is detectable up to 36 hours post feeding [38]. For arboviruses, the detection window may
222 be longer. For example, one study showed a reduction in DENV-2 RNA signal as early as 12
223 hours post-feeding, with little to no signal detected after 24 hours. However, if the virus
224 successfully replicated in mosquito tissues, a subsequent increase in RNA levels was
225 observed between 100 and 200 hours post-blood meal [38]. The co-detection of human DNA
226 and DENV RNA in the same mosquito pools suggests a common source, likely a viremic
227 human host. Although detection of DENV RNA does not necessarily indicate the presence of
228 infectious virions, its presence in two of these pools (K4 and V3) strongly suggests active
229 DENV circulation in these communities.

230 In addition to DENV, we identify reads mapping to *bat faecal associated dicistrovirus 4*.
231 Detection of this non-arbovirus might be related to incomplete degradation of the viral
232 material by the mosquito digestive system at the time of sampling. This is the first report of
233 *bat faecal associated dicistrovirus 4* in the DRC. While dicistrovirus is believed to exclusively
234 infect invertebrates, it has been recently reported in blood samples from febrile patients in
235 Tanzania and Nigeria [40,41], the intestinal content of a captive red squirrel with enteritis [42], and
236 has been identified in free-living gorillas in neighboring Republic of Congo [43]. Interestingly,
237 we found *bat faecal associated dicistrovirus 4* reads in a mosquito pool (K2) that exclusively

238 fed on human blood, suggesting that it came from an infected human. However, the host
239 range and pathogenicity of these viruses are unclear.

240 Our findings also shed light on circulating *Aedes* species along the DRC-Angola border.
241 Kimpese comprises a small city and surrounding region where more than 100,000 people
242 are thought to live [44], though the DRC has not performed a formal census since the 1950s. It
243 is located in the Kongo Central province, has a tropical climate, and spans mountains,
244 valleys, and grasslands. *Aedes aegypti* and *Ae. albopictus* are the main vectors of several
245 major pathogenic arboviruses, with *Ae. aegypti* being more competent for DENV and ZIKV
246 transmission [45]. *Ae. aegypti* was previously the dominant *Aedes* species in the DRC, until
247 recent, rapid replacement of native *Aedes* species by *Ae. albopictus* in the western and
248 northern regions of DRC [15]. Our findings corroborate these changes in the DRC *Aedes*
249 population; most collected *Aedes sp.* mosquitoes are *Ae. albopictus* (98.3%). The highly
250 diverse viromes in our *Aedes* mosquito pools include viruses specific to invertebrates,
251 vertebrates, plants, bacteria, fungi, and protozoa. These reads likely reflect the mosquitoes'
252 ingestion of blood, nectar, and environment substrates [46]. However, the large number of
253 unclassified reads within all pools confirms how much remains to be learned about this
254 important mosquito population.

255 Clustering observed among the samples from Kimpese city and Viaza in PCA provides
256 evidence of geographical differences in local *Aedes* mosquito populations. Most of the top
257 viral genera contributing to the variance in principal components 1 and 2 have been detected
258 in insects, plants, and bacteria. These findings suggest that local ecological and
259 environmental factors—such as elevation, land use patterns, or vegetation—may be shaping
260 the mosquito virome. In addition, the variability observed between mosquito pools within
261 Kimpese city may reflect microenvironmental differences or heterogeneous exposure to viral
262 sources within an urban landscape.

263 Several limitations of our study should be highlighted. First, mosquitoes were not pooled
264 based on morphological mosquito species. Second, our metagenomic analysis focuses on
265 *Aedes*. Analysis of other mosquito genera would provide broader insights into differences in
266 arboviral transmission and viromes in the DRC. Third, downsampling was necessary to
267 accommodate sequencing costs. We sequence a small number of mosquito pools from sites
268 within one region, which provides useful insights into arboviral transmission in Kimpese but
269 limits the generalizability of our findings to other regions. Fourth, despite positive RT-PCR
270 results and the identification of reads mapping to limited regions of the DENV genome, our
271 attempts to amplify additional and longer DENV fragments using several published assays
272 were unsuccessful, likely due to low RNA concentration and RNA degradation within the

273 mosquito. As a result, we did not have sufficient genomic coverage to construct whole
274 genomes. Nor can metagenomic sequencing tell us whether infectious virions are present or
275 definitively determine dengue types in circulation. Fifth, the use of mosquito pools improved
276 the yield of our sequencing efforts but prevents us from estimating the prevalence of viruses
277 in individual mosquitoes. Finally, viral metagenomic techniques have high sensitivity but low
278 specificity. To overcome this shortcoming, we employ a conservative approach leveraging
279 multiple bioinformatic tools complemented by real-time PCR, both of which confirm the
280 presence of DENV in our sample set.

281 In conclusion, our study provides new insights into viruses infecting *Aedes* in the DRC and
282 demonstrates the potential of wild-caught mosquito xenosurveillance. We use virome and
283 blood-meal analysis to improve understanding of *Aedes* mosquito feeding behavior in the
284 DRC, and present evidence of endemic DENV transmission in the Kimpese region near the
285 DRC's border with Angola. These findings are particularly relevant to ongoing discussions
286 about where to offer newly approved dengue vaccines and indicate a need for larger human
287 studies to define dengue epidemiology in the DRC and across Africa [47]. They also suggest a
288 role for sustained vector control efforts targeting *Aedes* in the DRC, extending beyond
289 outbreak response, and highlight opportunities for future arthropod-borne disease studies in
290 the region.

291 **Methods**

292 **Mosquito collection**

293 Adult *Aedes* mosquitoes were collected from three health areas in Kimpese, DRC, Ceco
294 (Kimpese city), Malanga, and Viaza (**Figure 2a**), using electric aspirators (Prokopack
295 Aspirator, John W. Hock, Gainesville, USA) and BG sentinel traps (Biogents Inc,
296 Regensburg, Germany) baited with dry ice. Mosquitoes were collected from April 23 - 30,
297 2022, during the rainy season when mosquito density is high. All collections were performed
298 outdoors, and GPS coordinates along with a brief description of collection sites were
299 recorded.

300 Collected mosquitoes were morphologically identified to the species level following the
301 Huang morphological key [48]. *Aedes* species were pooled by sample collection site. All field
302 mosquito pools were preserved in DNA/RNA Shield (ZYMO research, CA, USA) and stored
303 at -80°C.

304 Uninfected *Aedes aegypti* mosquitoes (NR-48920) were obtained from the NIH/NIAID
305 Filariasis Research Reagent Resource Center through BEI Resources. A random subset of
306 20 mosquitoes was pooled to serve as the laboratory uninfected *Ae. aegypti* control.

307 **Nucleic acid extraction**

308 Eight field *Aedes* mosquito pools, comprising a total of 155 mosquitoes, were randomly
309 selected from the three health areas: five from Kimpese city, one from Malanga, and two
310 from Viaza (**Figure 2b**). These pools represent approximately 20% of the total mosquito
311 pools from each region. The selected mosquito pools were washed with 70% ethanol and
312 rinsed twice with molecular-grade water before removal of mosquito heads [49]. Total RNA
313 was extracted from mosquito bodies from the selected field mosquito pools, the laboratory
314 un-infected *Ae. aegypti* mosquito pool from BEI Resources, and one water control using the
315 Quick-RNA Tissue/Insect kit (ZYMO research, CA, USA) following the manufacturer's
316 instructions. DNase I treatment using DNase I Set (ZYMO research, CA, USA) was carried
317 out during the RNA extraction process.

318 **Mosquito species confirmation and blood meal investigation**

319 To confirm the mosquito species, two regions within the cytochrome c oxidase I (*COI*), and
320 one region within the second internal transcribed spacer (*ITS2*) genes were amplified from
321 RNA extracted from the mosquito pools using published primers and conditions as shown in
322 **Table S9** [50–52]. DNA-based methods have been widely used in mosquito blood meal analysis
323 and provide reliable results [53]. The 16S ribosomal RNA (*16S*) and cytochrome *b* (*cytB*)
324 genes are commonly used due to their species-specific resolution [54,55]. In this study, we
325 amplified *16S* and *cytB* from RNA extracted from field-collected mosquito pools using
326 published primers (**Table S9**) [56,57]. All amplicons from the same mosquito pool were
327 combined in equimolar amounts. Then, 68 ng of DNA from each pooled amplicon was used
328 for library construction. Amplicon libraries were constructed using the Native Barcoding Kit
329 96 V14 and sequenced on a Flongle Flow Cell (R10.4.1) using the MinION platform (Oxford
330 Nanopore Technologies, Oxford, United Kingdom).

331 **Ribosomal RNA depletion, library preparation, and viral metagenomic sequencing**

332 To increase viral metagenomic sequencing efficiency, mosquito ribosomal RNA (rRNA)
333 depletion was carried out before library preparation using the NEBNext RNA Depletion Core
334 Reagent set (New England BioLabs, MA, USA) with published probes targeting *Aedes*
335 mosquitoes [58]. RNA fragment lengths after rRNA depletion were assessed for five pools
336 using Agilent TapeStation 4150 with High Sensitivity RNA ScreenTape (Agilent, Waldbronn,
337 Germany). Sequencing libraries were prepared and barcoded using the NEBNext Ultra II
338 Directional RNA Library Prep Kit and the Multiplex Oligos for Illumina (96 Unique Dual Index
339 Primer Pairs) kit (New England BioLabs, Massachusetts, USA), respectively. The barcoded
340 libraries were sequenced using the NovaSeq S4 platform (Illumina, California, USA) at the

341 High-Throughput Sequencing Facility (HTSF) at the University of North Carolina at Chapel
342 Hill to generate 150 bp paired-end reads. The expected total yield was 4-5 billion reads.

343 **Dengue virus confirmation by real-time PCR**

344 To confirm DENV calls made by sequencing, we tested RNA from all mosquito pools using a
345 published real-time PCR assay to detect pan-DENV RNA with the SuperScript III Platinum
346 One-Step qRT-PCR kit (Life Technologies, Carlsbad, CA, USA) [59].

347 **Data analysis**

348 To investigate viruses in the mosquito pools, Illumina NovaSeq sequencing reads were
349 demultiplexed into individual samples based on their barcode sequences. Paired-end reads
350 were then merged into single reads based on overlap detection using `BBMerge` (version
351 38.96) [60], followed by adapter removal using `Trimmomatic` (version 0.36) with default
352 parameters, and filtering short reads by setting the minimum length as 36 [61]. Reads mapping
353 to human (GRCh38.p14), *Ae. albopictus* (Aalbo_primary.1), and *Ae. aegypti* (AaegL5.0)
354 genomes, as well as the *Ae. simpsoni* CO1 gene (KT881399.1) were removed using `bwa-`
355 `mem2` (version 2.2.1) [62] and `SAMtools` (version 1.21) [63].

356 Reads remaining in the laboratory un-infected *Ae. aegypti* mosquito pool and water control
357 pool were assembled into contigs using `metaSPAdes` (version 4.0.0) with default
358 parameters [64]. These contigs were considered as contaminating contigs. Reads in field
359 mosquito pools were aligned to the contaminating contigs using `bwa-mem2` (version 2.2.1),
360 and mapping reads were removed using `SAMtools` (version 1.21). Taxonomic classification
361 of the remaining reads were performed using `KrakenUniq` (version 1.0.4) in default mode,
362 with the standard NCBI-nt database downloaded on July 31, 2023 [65]. Then, reads from field
363 mosquitoes mapping to sequences annotated as viral genera present in the laboratory
364 uninfected *Ae. aegypti* mosquito pool and water control were excluded from the analysis. A
365 viral genus or family was considered present by KrakenUniq if it had at least 10 mapped
366 reads per million viral reads based on the KrakenUniq reports using the default NCBI-nt
367 database [26]. If the total read count of a specific viral genus or family in a specific library is
368 less than 0.1% of the highest read count for that viral genus or family within the same
369 sequencing lane, then it was considered as a false-positive due to index-hopping [66]. The
370 relative abundance of viral genera and families was calculated based on the KrakenUniq
371 reports with default NCBI-nt database. This was done by dividing the number of reads
372 mapping to specific taxonomic groups by the total number of viral reads, then multiplying the
373 result by 100. Reads classified as viruses were extracted for further analysis. Principal
374 component analysis (PCA) was performed based on the viral genus annotation.

375 BLAST (version 2.14.1), an alignment-based method, was used to confirm the classification
376 of reads mapping to human and animal pathogens, as well as potential pathogens. BLAST-
377 confirmed reads mapping to human and animal pathogens or potential pathogens were
378 assembled into contigs using `metaSPAdes` (version 4.0.0) with default parameters. The
379 longest contigs or consensus sequences generated from merged paired-end reads for
380 pathogens and potential pathogens in the detected pools were selected and aligned with
381 representative reference sequences (**Table S10-S15**) from NCBI Virus, RefSeq, as well as
382 GenBank databases, including diverse genotypes/serotypes spanning multiple geographic
383 regions and collection years, using `MAFFT` (version 7.490) with default parameters.
384 Phylogenetic trees were generated using the maximum likelihood (ML) method in `RAxML-NG`
385 (version 1.2.2) [67], with the best-fit available model selected based on the Bayesian
386 Information Criterion (BIC) values in `IQ-TREE` (version 2.4.0) [68].

387 For Nanopore sequencing data used for mosquito species determination and blood meal
388 analysis, raw data in Fast5 file format from the sequencer were used for base-calling with
389 Guppy (version 5.6.7), with a phred quality score ≥ 6 (Q score ≥ 6). Reads were
390 demultiplexed according to their barcodes, which were then trimmed using Guppy with
391 defaults. BLAST was applied to all passed reads to investigate the mosquito species and
392 blood sources (calls were made for hits with e-value < 1e-6 and length > 100bp).

393 All data was visualized in R software (version 4.2.0; R Core Team, Vienna, Austria) in
394 RStudio (version 2022.02.2) with *ggrepel* (version 0.9.6), *ggplot2* (version 3.5.2), *tidyverse*
395 (version 2.0.0), *eulerr* (version 7.0.2), *viridis* (version 0.6.5), *scico* (version 1.5.0), *ape*
396 (version 5.8-1), *ggtree* (version 3.16.0), *rentrez* (version 1.2.4), *countrycode* (version 1.6.1),
397 *RColorBrewer* (version 1.1-3), and *dplyr* (version 1.1.4) packages. Mapping was done using
398 *sf* (version 1.0.21), *rnaturalearth* (version 1.0.1), and *rnaturalearthdata* (version 1.0.0)
399 packages in R software. Data for mapping was downloaded from the Global Administrative
400 Areas Database (GADM) [69] and the Humanitarian Data Exchange (HDX) [70].

401 Acknowledgements

402 We thank Daniel Neafsey for sharing mosquito blood meal sequencing protocols and advice.
403 The following reagent was provided by the NIH/NIAID Filariasis Research Reagent
404 Resource Center for distribution through BEI Resources, NIAID, NIH: Uninfected *Aedes*
405 *aegypti*, Strain Black Eye Liverpool (Frozen), NR-48920.

The authors used an artificial intelligence language model for English language editing during the writing process. However, the manuscript is original to the authors, who take responsibility for its content.

Author contributions

W.H., J.J.J, and J.B.P. conceptualized the study and designed experiments. T.B. and F.V. collected field mosquito samples. M.M.K. and A.K.T. helped coordinate these collections. W.H. performed laboratory tests. W.H., A.P., Z.R.P.-H., and M.H.C. performed data analyses. W.H. prepared the figures and wrote the first draft. All authors reviewed and approved the final draft.

Funding

Mosquito collection was funded by a Yang Biomedical Scholar award from University of North Carolina (JJJ). This work was supported in part by NIAID K24AI134990 (JJJ), funds from the UNC Office for Research (JBP), and the Bill & Melinda Gates Foundation (INV-050353 to JBP). Under the grant conditions of the Foundation, a Creative Commons Attribution 4.0 Generic License has already been assigned to the Author Accepted Manuscript version that might arise from this submission.

Competing interests

JBP reports research support from Gilead Sciences, non-financial support from Abbott Laboratories, and past consulting for Zymeron Corporation, all outside the scope of the current manuscript.

Data availability

NovaSeq and MinION sequencing data presented in the study are deposited in the NCBI Sequence Read Archive (BioProject ID: PRJNA1200724 and PRJNA1200731).

Code availability

Analysis code is publicly available at https://github.com/IDEELResearch/DRCAedesSeq.

References

1. Vector-borne diseases. https://www.who.int/news-room/fact-sheets/detail/vector-borne-diseases.
2. Kading, R. C., Brault, A. C. & Beckham, J. D. Global Perspectives on Arbovirus Outbreaks: A 2020 Snapshot. *Trop Med Infect Dis* **5**, (2020).
3. Mbanzulu, K. M. *et al.* Mosquito-borne viral diseases in the Democratic Republic of the Congo: a review. *Parasit. Vectors* **13**, 103 (2020).
4. Burt, F. J. *et al.* Chikungunya virus: an update on the biology and pathogenesis of this emerging pathogen. *Lancet Infect. Dis.* **17**, e107–e117 (2017).
5. Tajudeen, Y. A., Oladunjoye, I. O., Mustapha, M. O., Mustapha, S. T. & Ajide-Bamigboye, N. T. Tackling the global health threat of arboviruses: An appraisal of the three holistic approaches to health. *Health Promot Perspect* **11**, 371–381 (2021).
6. Chala, B. & Hamde, F. Emerging and re-emerging vector-borne infectious diseases and the challenges for control: A review. *Front. Public Health* **9**, 715759 (2021).
7. Bobanga, T., Moyo, M., Vulu, F. & Irish, S. R. First Report of *Aedes albopictus* (Diptera: Culicidae) in the Democratic Republic of Congo. *Afr. Entomol.* **26**, 234–236 (2018).
8. Poungou, N. *et al.* Mosquito-Borne Arboviruses Occurrence and Distribution in the Last Three Decades in Central Africa: A Systematic Literature Review. *Microorganisms* **12**, (2023).
9. Janjoter, S., Kataria, D., Yadav, M., Dahiya, N. & Sehrawat, N. Transovarial transmission of mosquito-borne viruses: a systematic review. *Front. Cell. Infect. Microbiol.* **13**, 1304938 (2023).
10. Renard, A. *et al.* Interaction of Human Behavioral Factors Shapes the Transmission of Arboviruses by Aedes and Culex Mosquitoes. *Pathogens* **12**, (2023).
11. Kraemer, M. U. *et al.* The global distribution of the arbovirus vectors and. *Elife* **4**, (2015).
12. Shikanda, H. WHO prequalifies new dengue vaccine, but Africa still not in the picture. *Nation* https://nation.africa/kenya/health/who-prequalifies-new-dengue-vaccine-but-africa-still-not-in-the-picture-4626442 (2024).
13. Foley, D. H., Rueda, L. M. & Wilkerson, R. C. Insight into global mosquito biogeography from country species records. *J. Med. Entomol.* **44**, 554–567 (2007).
14. Manzambi, E. Z. *et al.* Behavior of Adult Aedes aegypti and Aedes albopictus in Kinshasa, DRC, and the Implications for Control. *Trop. Med. Infect. Dis.* **8**, (2023).
15. Vulu, F. *et al.* Geographic expansion of the introduced Aedes albopictus and other native Aedes species in the Democratic Republic of the Congo. *Parasit. Vectors* **17**, 35 (2024).
16. Otshudiema, J. O. *et al.* Yellow Fever Outbreak - Kongo Central Province, Democratic Republic of the Congo, August 2016. *MMWR Morb. Mortal. Wkly. Rep.* **66**, 335–338 (2017).
17. Willcox, A. C. *et al.* Seroepidemiology of Dengue, Zika, and Yellow Fever Viruses among Children in the Democratic Republic of the Congo. *Am. J. Trop. Med. Hyg.* **99**, 756–763 (2018).
18. Selhorst, P. *et al.* Molecular characterization of chikungunya virus during the 2019 outbreak in the Democratic Republic of the Congo. *Emerg. Microbes Infect.* **9**, 1912–

474 1918 (2020).

475 19. Mbanzulu, K. M. *et al.* Mosquito-borne viruses circulating in Kinshasa, Democratic
476 Republic of the Congo. *Int. J. Infect. Dis.* **57**, 32–37 (2017).

477 20. Sendor, R. *et al.* Epidemiology of Plasmodium malariae and Plasmodium ovale spp. in
478 Kinshasa Province, Democratic Republic of Congo. *Nat. Commun.* **14**, 6618 (2023).

479 21. Messina, J. P. *et al.* The current and future global distribution and population at risk of
480 dengue. *Nat Microbiol* **4**, 1508–1515 (2019).

481 22. Kajeguka, D. C. *et al.* Prevalence of dengue and chikungunya virus infections in north-
482 eastern Tanzania: a cross sectional study among participants presenting with malaria-
483 like symptoms. *BMC Infect. Dis.* **16**, 183 (2016).

484 23. Bernadus, J. B. B. *et al.* Metagenomic Insight into the Microbiome and Virome
485 Associated with Aedes aegypti Mosquitoes in Manado (North Sulawesi, Indonesia).
486 *Infect. Dis. Rep.* **15**, 549–563 (2023).

487 24. Gangopadhayya, A. *et al.* Metagenomic Analysis of Viromes of Aedes Mosquitoes
488 across India. *Viruses* **16**, (2024).

489 25. Pan, Y.-F. *et al.* Metagenomic analysis of individual mosquito viromes reveals the
490 geographical patterns and drivers of viral diversity. *Nat Ecol Evol* **8**, 947–959 (2024).

491 26. Wang, Y. *et al.* Metagenomic sequencing reveals viral diversity of mosquitoes from
492 Shandong Province, China. *Microbiol Spectr* e0393223 (2024).

493 27. Postler, T. S. *et al.* Renaming of the genus Flavivirus to Orthoflavivirus and extension of
494 binomial species names within the family Flaviviridae. *Arch. Virol.* **168**, (2023).

495 28. Meng, J.-X. *et al.* Isolation and genetic evolution of dengue virus from the 2019 outbreak
496 in Xishuangbanna, Yunnan Province, China. *Vector Borne Zoonotic Dis.* **23**, 331–340
497 (2023).

498 29. Vogels, C. B. F. *et al.* DengueSeq: a pan-serotype whole genome amplicon sequencing
499 protocol for dengue virus. *BMC Genomics* **25**, 433 (2024).

500 30. Fraenkel, S. *et al.* The development of new primer sets for the amplification and
501 sequencing of the envelope gene of all dengue virus serotypes. *Microorganisms* **12**,
502 1092 (2024).

503 31. Rahman, A. *et al.* Unveiling ancestral relations, host–pathogen interactions and
504 comparative viral miRNA insights of dengue virus serotypes. *Network Modeling Analysis*
505 *in Health Informatics and Bioinformatics* **10**, 27 (2021).

506 32. Yung, C.-F. *et al.* Dengue serotype-specific differences in clinical manifestation,
507 laboratory parameters and risk of severe disease in adults, singapore. *Am. J. Trop.*
508 *Med. Hyg.* **92**, 999–1005 (2015).

509 33. Selhorst, P. *et al.* Phylogeographic analysis of dengue virus serotype 1 and
510 cosmopolitan serotype 2 in Africa. *Int. J. Infect. Dis.* **133**, 46–52 (2023).

511 34. Garamszegi, L. Z. Host diversity of Aedes albopictus in relation to invasion history: a
512 meta-analysis of blood-feeding studies. *Parasit. Vectors* **17**, 411 (2024).

513 35. Tchouassi, D. P. *et al.* Next generation sequencing improves the resolution of detecting
514 mixed host blood meal sources in field collected arboviral mosquito vectors. *Med. Vet.*
515 *Entomol.* **38**, 407–415 (2024).

516 36. Almeida, P. R. de, Weber, M. N., Sonne, L. & Spilki, F. R. Aedes-borne orthoflavivirus
517 infections in neotropical primates - Ecology, susceptibility, and pathogenesis. *Exp. Biol.*

518 *Med.* **248**, 2030–2038 (2023).

519 37. Hiroshige, Y. *et al.* A human genotyping trial to estimate the post-feeding time from
520 mosquito blood meals. *PLoS One* **12**, e0179319 (2017).

521 38. Drummond, C. *et al.* Stability and detection of nucleic acid from viruses and hosts in
522 controlled mosquito blood feeds. *PLoS One* **15**, e0231061 (2020).

523 39. Grubaugh, N. D. *et al.* Xenosurveillance: a novel mosquito-based approach for
524 examining the human-pathogen landscape. *PLoS Negl. Trop. Dis.* **9**, e0003628 (2015).

525 40. Cordey, S. *et al.* Detection of dicistroviruses RNA in blood of febrile Tanzanian children.
526 *Emerg. Microbes Infect.* **8**, 613–623 (2019).

527 41. Oguzie, J. U. *et al.* Metagenomic surveillance uncovers diverse and novel viral taxa in
528 febrile patients from Nigeria. *Nat. Commun.* **14**, 4693 (2023).

529 42. Dastjerdi, A., Everest, D. J., Davies, H., Denk, D. & Zell, R. A novel dicistrovirus in a
530 captive red squirrel (Sciurus vulgaris). *J. Gen. Virol.* **102**, (2021).

531 43. Duraisamy, R. *et al.* Detection of novel RNA viruses from free-living gorillas, Republic of
532 the Congo: genetic diversity of picobirnaviruses. *Virus Genes* **54**, 256–271 (2018).

533 44. Fumwakwau, J. K., Derra, K., Nzolo, D. B., Mampunza, S. M. M. & Phanzu, D. M.
534 Cohort profile: Kimpese health and demographic surveillance system, democratic
535 republic of Congo. *Int. J. Epidemiol.* **53**, dyae150 (2024).

536 45. Sun, X. *et al.* Gut symbiont-derived sphingosine modulates vector competence in Aedes
537 mosquitoes. *Nat. Commun.* **15**, 8221 (2024).

538 46. Hameed, M. *et al.* A viral metagenomic analysis reveals rich viral abundance and
539 diversity in mosquitoes from pig farms. *Transbound. Emerg. Dis.* **67**, 328–343 (2019).

540 47. WHO position paper on dengue vaccines, May 2024.
541 https://www.who.int/publications/i/item/who-wer-9918-203-224.

542 48. Huang, Y.-M. *The Subgenus Stegomyia of Aedes in the Afrotropical Region with Keys*
543 *to the Species (Diptera: Culicidae)*. (Magnolia Press, 2004).

544 49. Phalen, H. *et al.* A Mosquito Pick-and-Place System for PfSPZ-based Malaria Vaccine
545 Production. *IEEE Trans. Autom. Sci. Eng.* **18**, 299–310 (2020).

546 50. Zhang, D. X. & Hewitt, G. M. Nuclear integrations: challenges for mitochondrial DNA
547 markers. *Trends Ecol. Evol.* **11**, 247–251 (1996).

548 51. Batovska, J., Blacket, M. J., Brown, K. & Lynch, S. E. Molecular identification of
549 mosquitoes (Diptera: Culicidae) in southeastern Australia. *Ecol. Evol.* **6**, 3001–3011
550 (2016).

551 52. Folmer, O., Black, M., Hoeh, W., Lutz, R. & Vrijenhoek, R. DNA primers for amplification
552 of mitochondrial cytochrome c oxidase subunit I from diverse metazoan invertebrates.
553 *Mol. Mar. Biol. Biotechnol.* **3**, 294–299 (1994).

554 53. Reeves, L. E. & Burkett-Cadena, N. D. Mosquito blood meal analysis. *Cold Spring Harb.*
555 *Protoc.* **2024**, db.top107706 (2024).

556 54. Ogola, E. *et al.* Composition of Anopheles mosquitoes, their blood-meal hosts, and
557 Plasmodium falciparum infection rates in three islands with disparate bed net coverage
558 in Lake Victoria, Kenya. *Malar. J.* **16**, 360 (2017).

559 55. Talebzadeh, F. *et al.* Efficiency of mitochondrial genes and nuclear Alu elements in
560 detecting human DNA in blood meals of Anopheles stephensi mosquitoes: a time-
561 course study. *Parasit. Vectors* **16**, 284 (2023).

562 56. Meyer, R., Höfelein, C., Lüthy, J. & Candrian, U. Polymerase chain reaction-restriction
563 fragment length polymorphism analysis: a simple method for species identification in
564 food. *J. AOAC Int.* **78**, 1542–1551 (1995).

565 57. Taylor, P. G. Reproducibility of ancient DNA sequences from extinct Pleistocene fauna.
566 *Mol. Biol. Evol.* **13**, 283–285 (1996).

567 58. Fauver, J. R. *et al.* A reverse-transcription/RNase H based protocol for depletion of
568 mosquito ribosomal RNA facilitates viral intrahost evolution analysis, transcriptomics
569 and pathogen discovery. *Virology* **528**, 181–197 (2018).

570 59. Waggoner, J. J. *et al.* Single-Reaction Multiplex Reverse Transcription PCR for
571 Detection of Zika, Chikungunya, and Dengue Viruses. *Emerg. Infect. Dis.* **22**, 1295–
572 1297 (2016).

573 60. Bushnell, B., Rood, J. & Singer, E. BBMerge - Accurate paired shotgun read merging
574 via overlap. *PLoS One* **12**, e0185056 (2017).

575 61. Bolger, A. M., Lohse, M. & Usadel, B. Trimmomatic: a flexible trimmer for Illumina
576 sequence data. *Bioinformatics* **30**, 2114–2120 (2014).

577 62. Vasimuddin, M., Misra, S., Li, H. & Aluru, S. Efficient Architecture-Aware Acceleration of
578 BWA-MEM for Multicore Systems. in *2019 IEEE International Parallel and Distributed*
579 *Processing Symposium (IPDPS)* 314–324 (IEEE, 2019).

580 63. Li, H. *et al.* The Sequence Alignment/Map format and SAMtools. *Bioinformatics* **25**,
581 2078–2079 (2009).

582 64. Nurk, S., Meleshko, D., Korobeynikov, A. & Pevzner, P. A. metaSPAdes: a new
583 versatile metagenomic assembler. *Genome Res.* **27**, 824–834 (2017).

584 65. Breitwieser, F. P., Baker, D. N. & Salzberg, S. L. KrakenUniq: confident and fast
585 metagenomics classification using unique k-mer counts. *Genome Biol.* **19**, 198 (2018).

586 66. Pan, Y.-F. *et al.* Metagenomic analysis of individual mosquitos reveals the ecology of
587 insect viruses. *bioRxivorg* (2023) doi:10.1101/2023.08.28.555221.

588 67. Kozlov, A. M., Darriba, D., Flouri, T., Morel, B. & Stamatakis, A. RAxML-NG: a fast,
589 scalable and user-friendly tool for maximum likelihood phylogenetic inference.
590 *Bioinformatics* **35**, 4453–4455 (2019).

591 68. Minh, B. Q. *et al.* IQ-TREE 2: New models and efficient methods for phylogenetic
592 inference in the genomic era. *Mol. Biol. Evol.* **37**, 1530–1534 (2020).

593 69. *Database of Global Administrative Areas (GADM) (2024). University of California,*
594 *Berkeley* http://www.gadm.org.

595 70. Welcome - Humanitarian Data Exchange. https://data.humdata.org/.

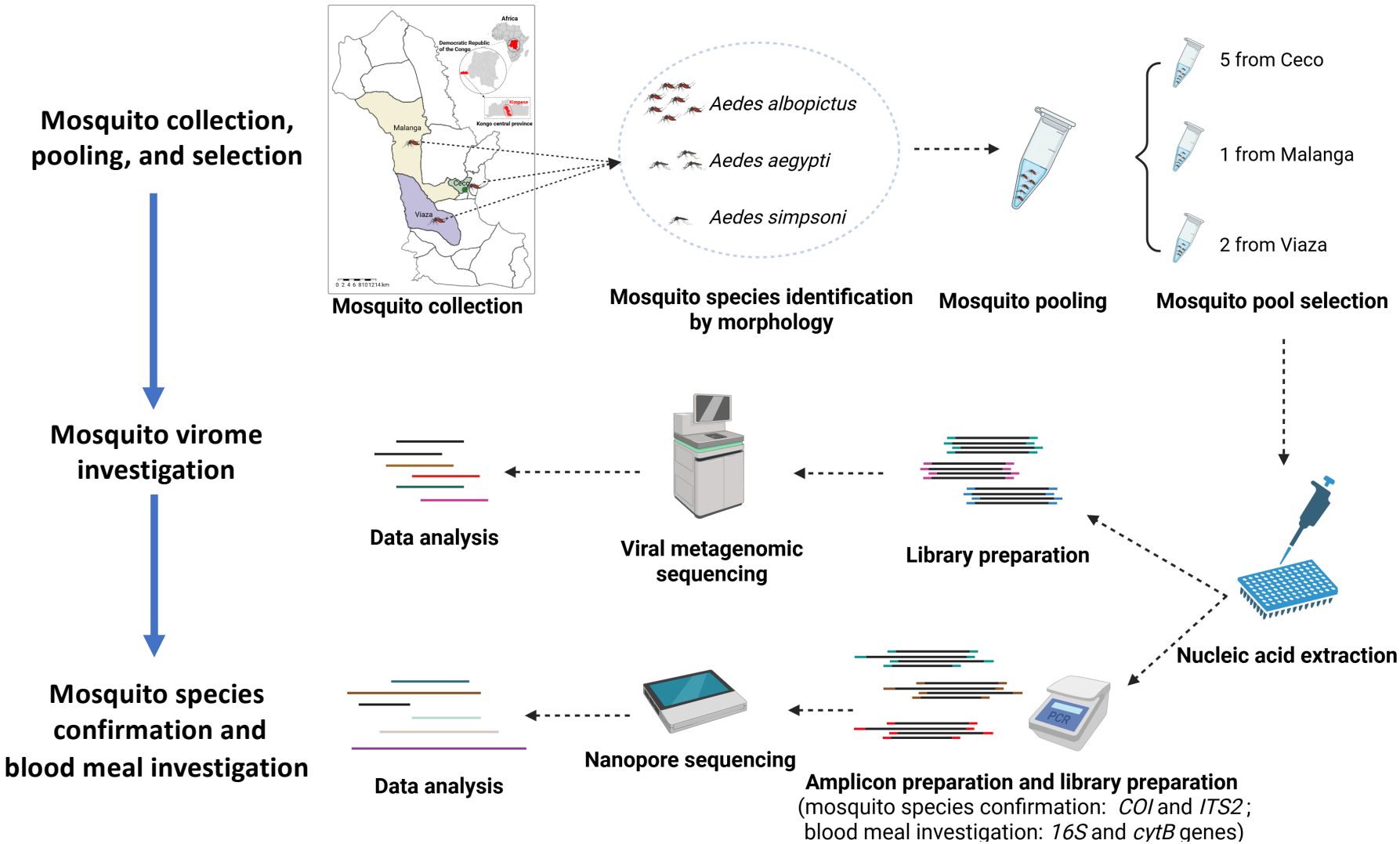

Figure 1. Schematic of the viral metagenomic, mosquito species, and blood meal analysis of *Aedes* mosquitoes from the Democratic Republic of the Congo. Created in BioRender.

(A)

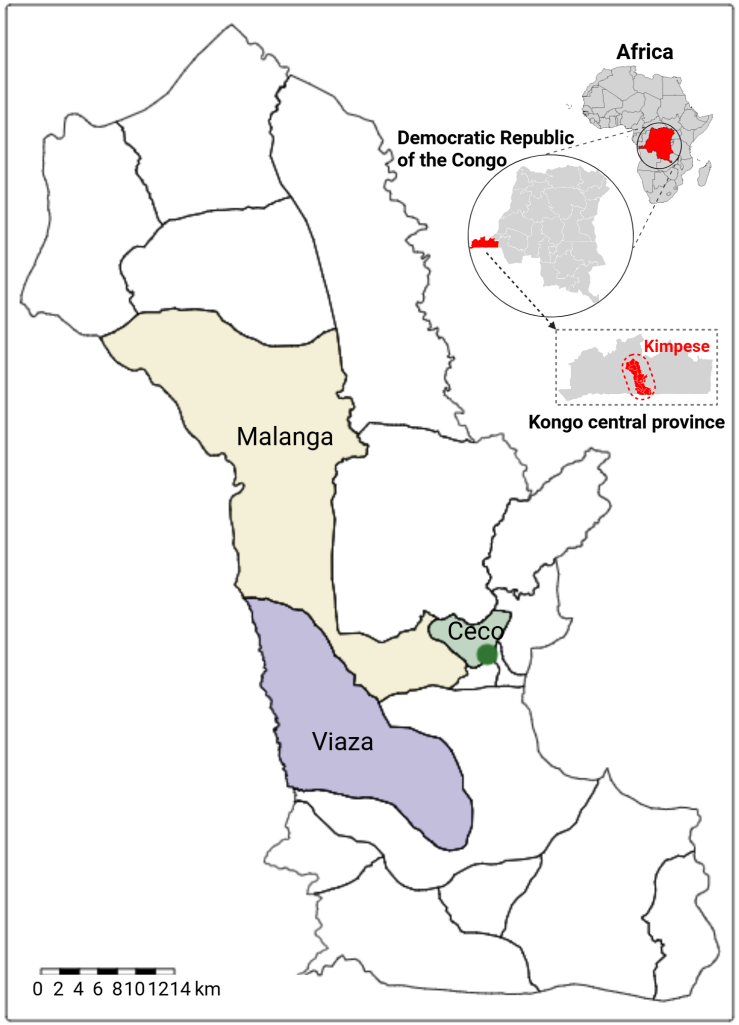

(B)

Sample collection site	Sample Name	Number of mosquitoes
Malanga	M_1	17
Viaza	V_2	13
Viaza	V_3	21
Ceco	K_1	34
Ceco	K_2	11
Ceco	K_3	9
Ceco	K_4	18
Ceco	K_5	32
Laboratory	Lab 1	20
H_2O	H_2O	NA

Figure 2. *Aedes* mosquitoes trapped in the DRC. A) Sample collection areas in Kimpese, DRC. Kimpese city is annotated by a green dot. B) Detailed information of the selected mosquito pools, including health areas where they were collected, and including laboratory-reared *Ae. aegypti* (Lab 1) and water (H_2O) controls.

(A)

Sample name	Raw reads, n	Reads merged, %	Trimmed, merged reads, n	Reads after filtering mosquito and human genomes, as well as contaminating contigs, n	Bacteria reads, n	Eukaryota reads, n	Archaea reads, n	Virus reads, n	Unclassified reads, n
K1	360,737,972	84.4	152,095,120	5,393,296	1,335,872	677,884	76	96,956	3,262,468
K2	398,414,652	81.0	161,174,765	2,030,364	706,544	68,852	100	2,472	1,250,728
K3	490,456,654	79.0	193,409,000	3,622,360	989,440	248,304	220	439,000	1,942,576
K4	533,539,492	82.2	219,026,312	27,282,152	11,335,312	7,467,640	6,196	1,207,424	6,797,388
K5	451,970,894	84.4	190,392,544	36,208,616	828,524	646,252	236	2,204,216	32,527,208
M1	425,890,652	84.1	218,983,230	53,989,214	235,418	926,940	428	1,316,904	50,567,428
V2	597,943,980	79.1	235,857,112	44,181,864	610,584	524,820	496	1,618,920	41,407,520
V3	536,292,608	78.2	209,150,864	12,913,872	1,934,060	706,500	532	3,555,364	6,714,520

(B)

Sample name	Vertebrate	Invertebrate	Plant	Bacteria	Fungi	Protozoa	Unclassified
K1	25784.9	789966.6	82.5	4125.6	206.3	0	179834.1
K2	124595.5	846278.3	3236.2	0	3236.2	1618.1	21035.7
K3	34077.4	534870.2	0	18.2	0	18.2	431016
K4	19280.7	536981.2	13.2	1593.5	0	0	442131.4
K5	5877.8	106211.0	0	47.2	0	74.4	887789.6
M1	3945.6	972444.5	42.5	5127.2	2035.0	0	16405.2
V2	19489.5	710999.9	14.8	49.4	51.9	0	269394.5
V3	20660.6	549702.4	0	0	0	0	429637

Figure 3. Summary of read counts based on the KrakenUniq nt database. A) Summary statistics for sequenced mosquito pools. **B)** Virus reads by presumed host, reported as reads per million based on KrakenUniq annotation using the nt database.

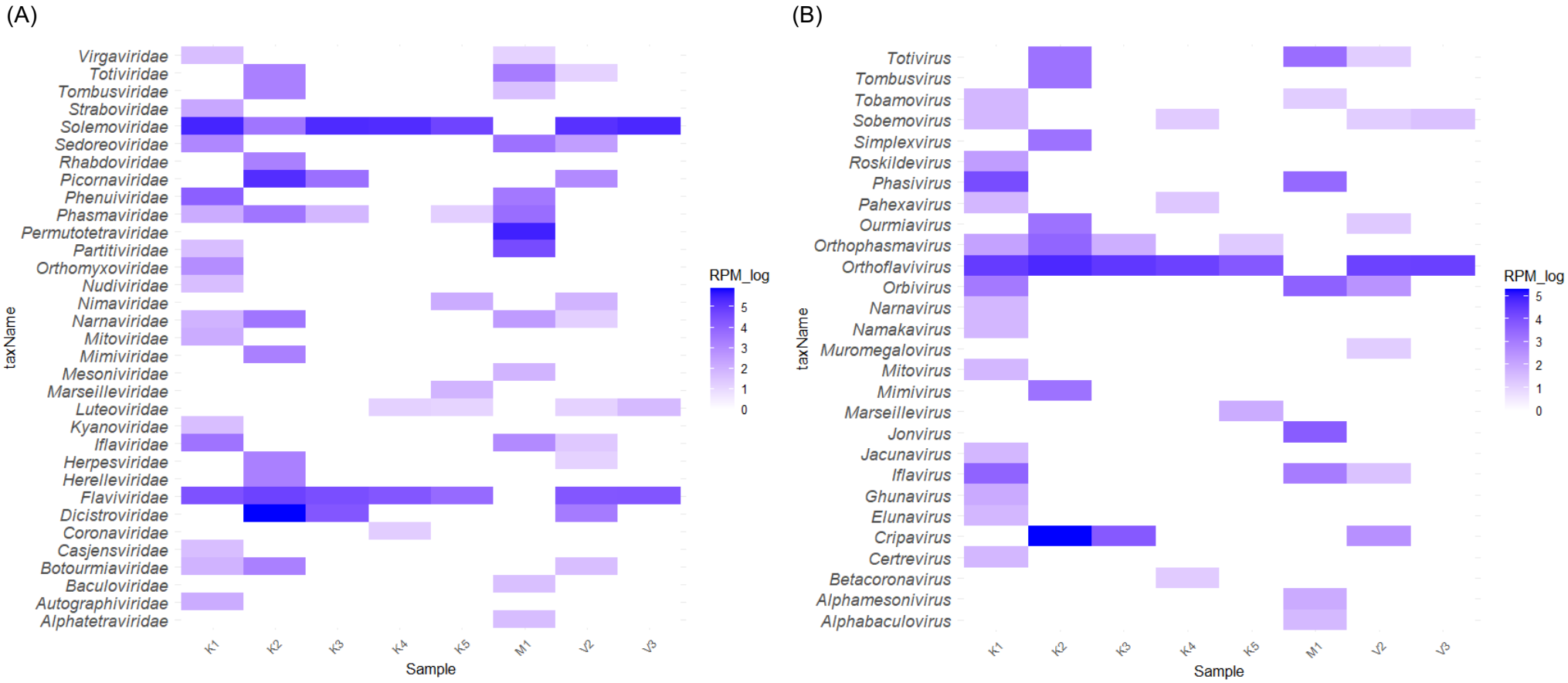

Figure 4. Viral families and genera in field mosquito pools. **A)** Heatmap based on reads per million viral reads in each mosquito pool (family level). **B)** Heatmap based on reads per million viral reads in each mosquito pool (genus level). Per International Committee on Taxonomy of Viruses recommendations, reads of *Orthoflavivirus* comprises both *Orthoflavivirus* and *Flavivirus* identified by KrakenUniq.

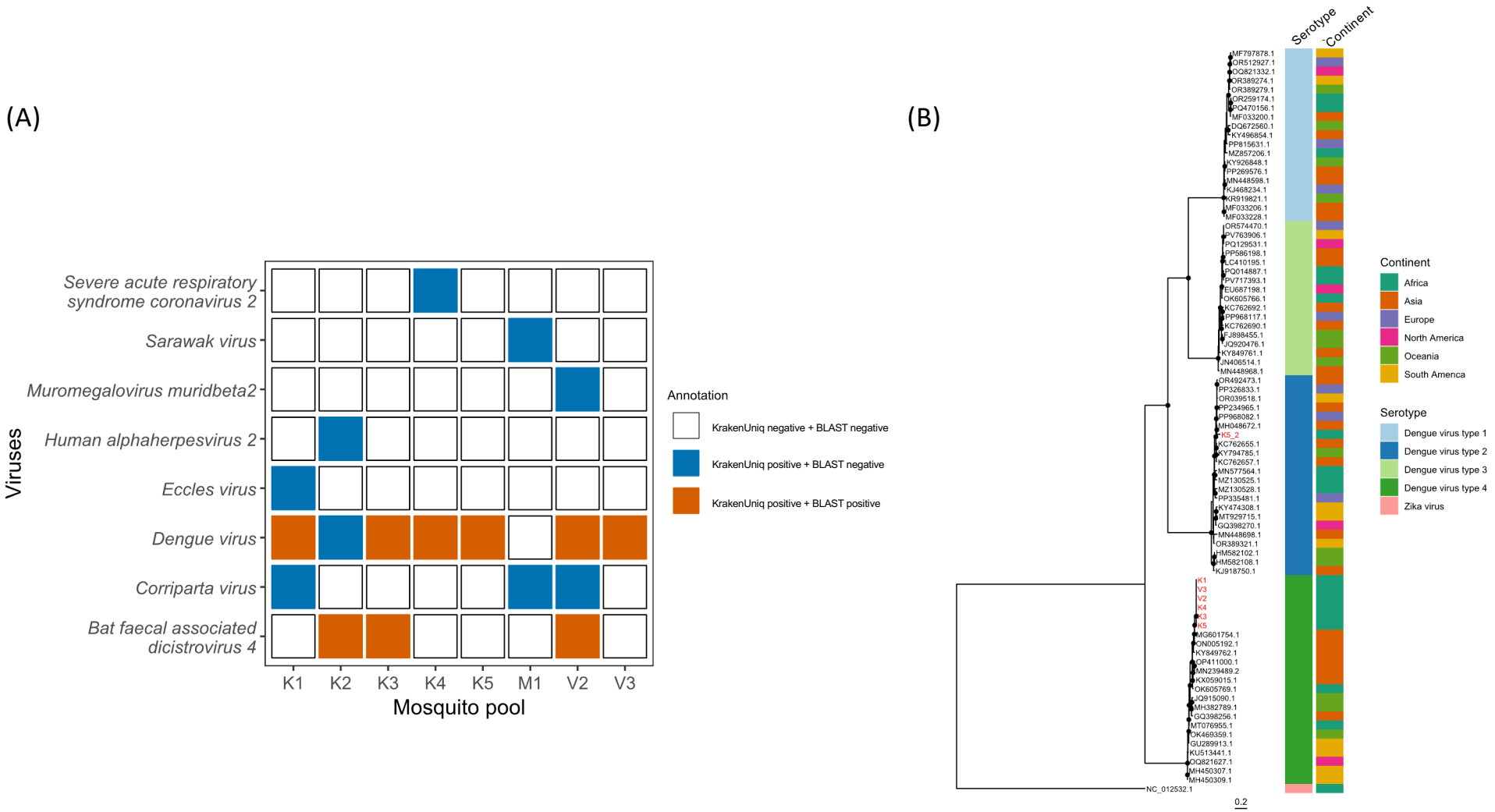

Figure 5. Known human or animal viruses detected in mosquito pools, and phylogenetic analysis of detected DENV RNA. A) Annotation results based on KrakenUniq with default nt database and BLAST are shown in different colors. Vermillion rectangulars signify confirmation by two methods used. **B)** Phylogenetic analysis of dengue reads from field mosquito pools. Maximum likelihood phylogenetic trees comparing DENV short reads (~ 100bp) from DRC mosquito pools (red) to reference sequences (black). The tree is constructed using RAxML-NG under the GTR+F+I+G4 model, with NC_012532.1 (Zika virus sequence) as the outgroup. Black dots indicate nodes with bootstrap support greater than 70% across 1,000 replicates.

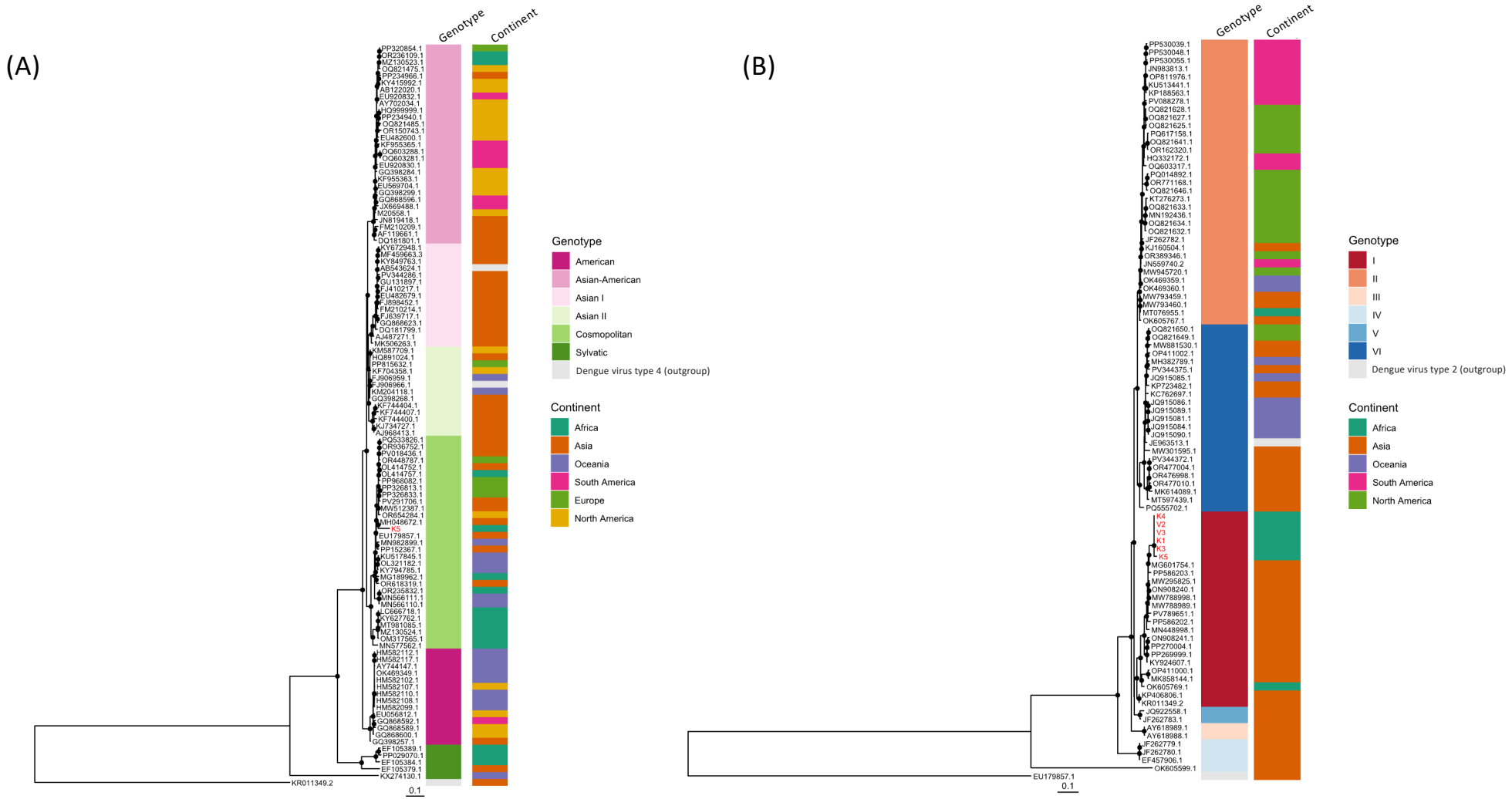

Figure 6. Phylogenetic analysis of DENV-2 and DENV-4 reads from field mosquito pools. Maximum likelihood phylogenetic trees comparing DENV reads from DRC mosquito pools (red) to reference sequences (black), constructed using RAxML-NG (GTR+F+I+G4 model) with KR011349.2 and EU179857.1 as outgroups, respectively. Analysis of the **A)** DENV-2 showing clustering of reads from a single DRC pool (mapping to non-coding region, ~100bp) with DENV-2 reference sequences (>10,000bp), though with limited bootstrap support. and **B)** DENV-4 showing clustering of reads from six DRC pools (mapping to non-coding region, ~100bp) with DENV-4 references sequences (>10,000bp). Black dots indicate nodes with bootstrap support greater than 70% based on 1,000 replicates.

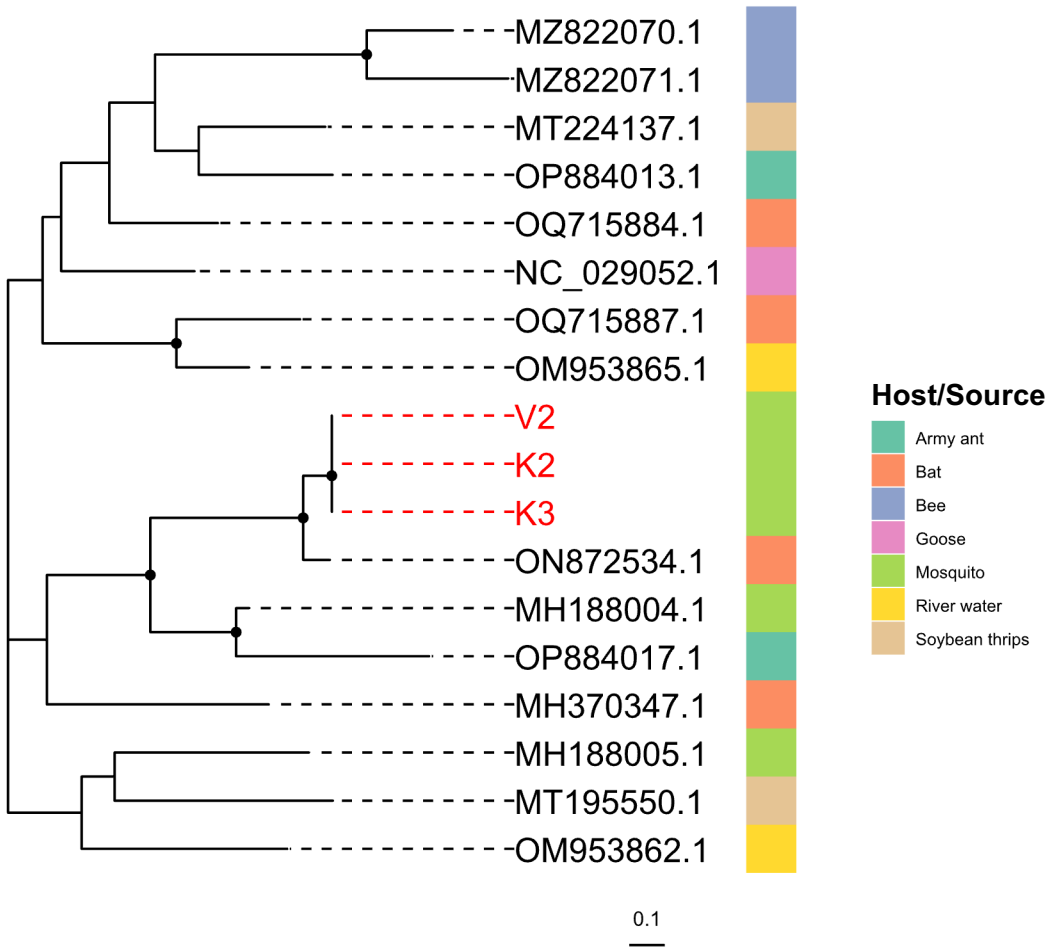

Figure 7. Phylogenetic analysis of bat faecal associated dicistrovirus 4 reads in DRC field mosquito pools (red) mapping to the non-coding region (7078 - 7330 nt based on ON872534.1) compared to published sequences (black), constructed using RAxML-NG with the HKY+F+G4 model. Black dots indicate nodes with bootstrap support greater than 70% across 1,000 replicates.

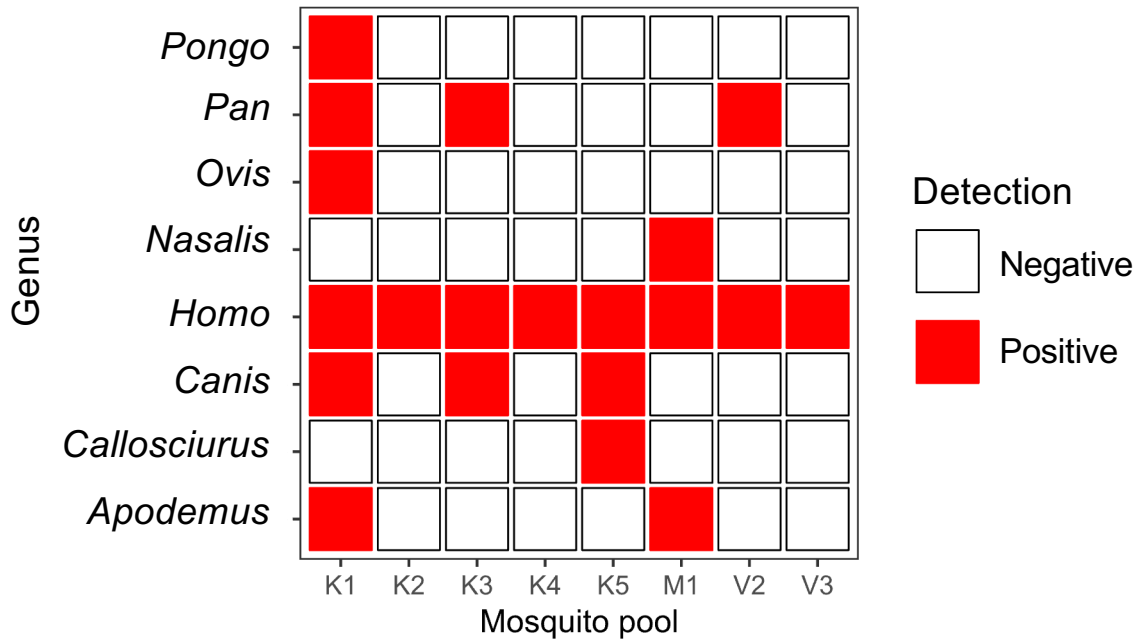

Figure 8. Mosquito blood meal sources determined by amplicon sequencing of the 16S ribosomal RNA and cytochrome b genes.

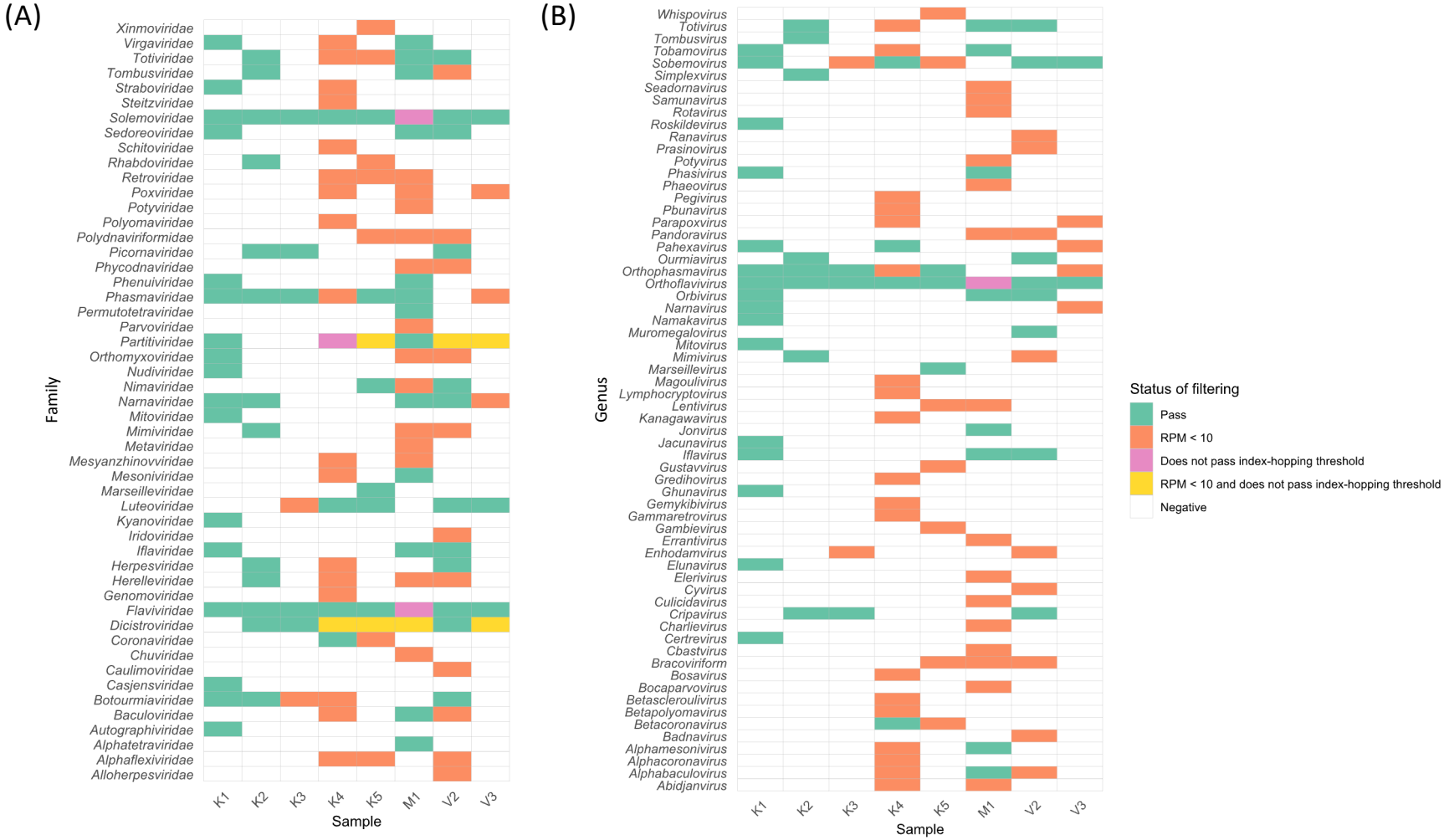

Figure S1. **Filtering results by viral family and genus.** After applying the RPM < 10 threshold and index-hopping filter, **A)** a total of 33 unique total viral families are detected, with each pool containing between 3-17 passed viral families, and **B)** a total of 28 unique total viral genera are detected, with each pool containing between 2-16 passed viral genera. Shaded cells have detected reads, with color denoting filtering result.

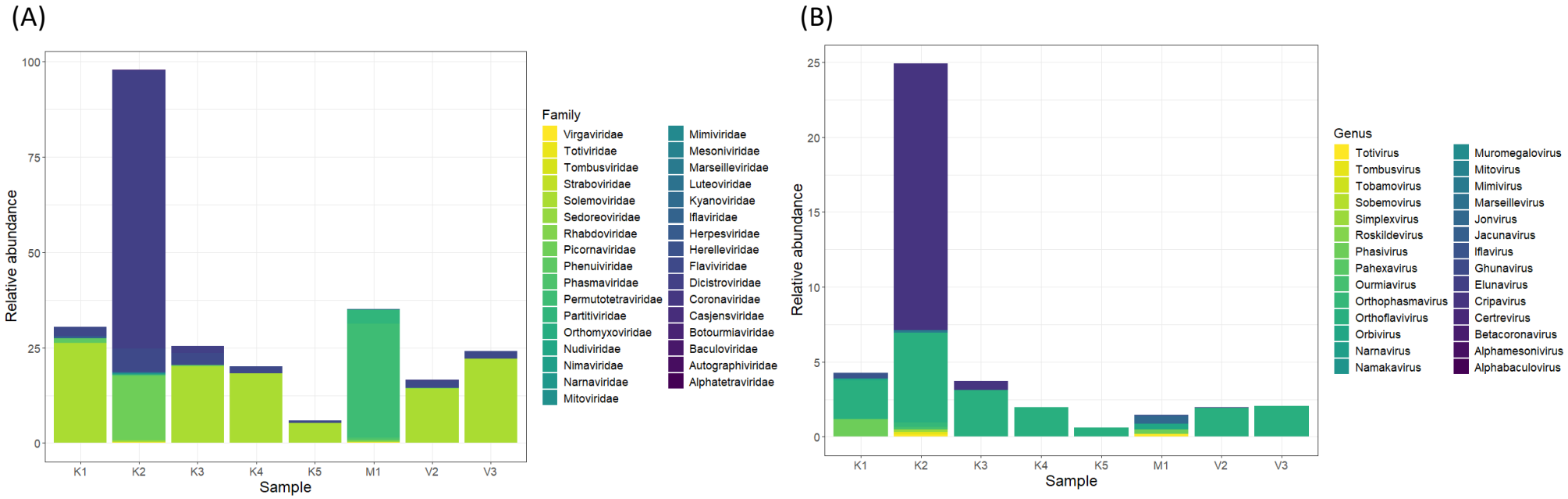

Figure S2. **Viral families and genera detected in field mosquito pools** (after filtering out those with <10 RPM or evidence of index-hopping). **A)** Top five families in each field mosquito pool. **B)** Top five genera in each field mosquito pool. Per International Committee on Taxonomy of Viruses recommendations, relative abundance of *Orthoflavivirus* comprises both *Orthoflavivirus* and *Flavivirus* identified by KrakenUniq.

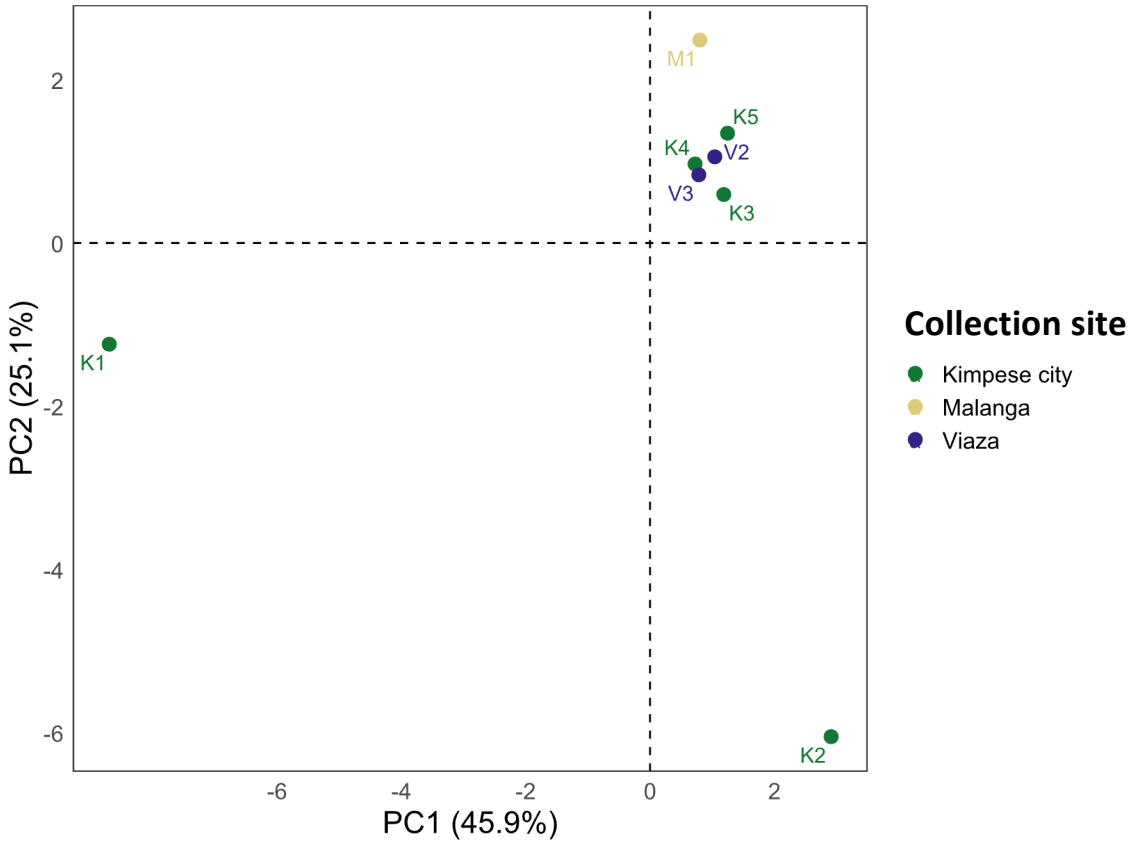

Figure S3. Principal component analysis (PCA) annotated by collection site using a data matrix containing relative abundance of viral genera (after applying the 10 RPM threshold and index-hopping filter).

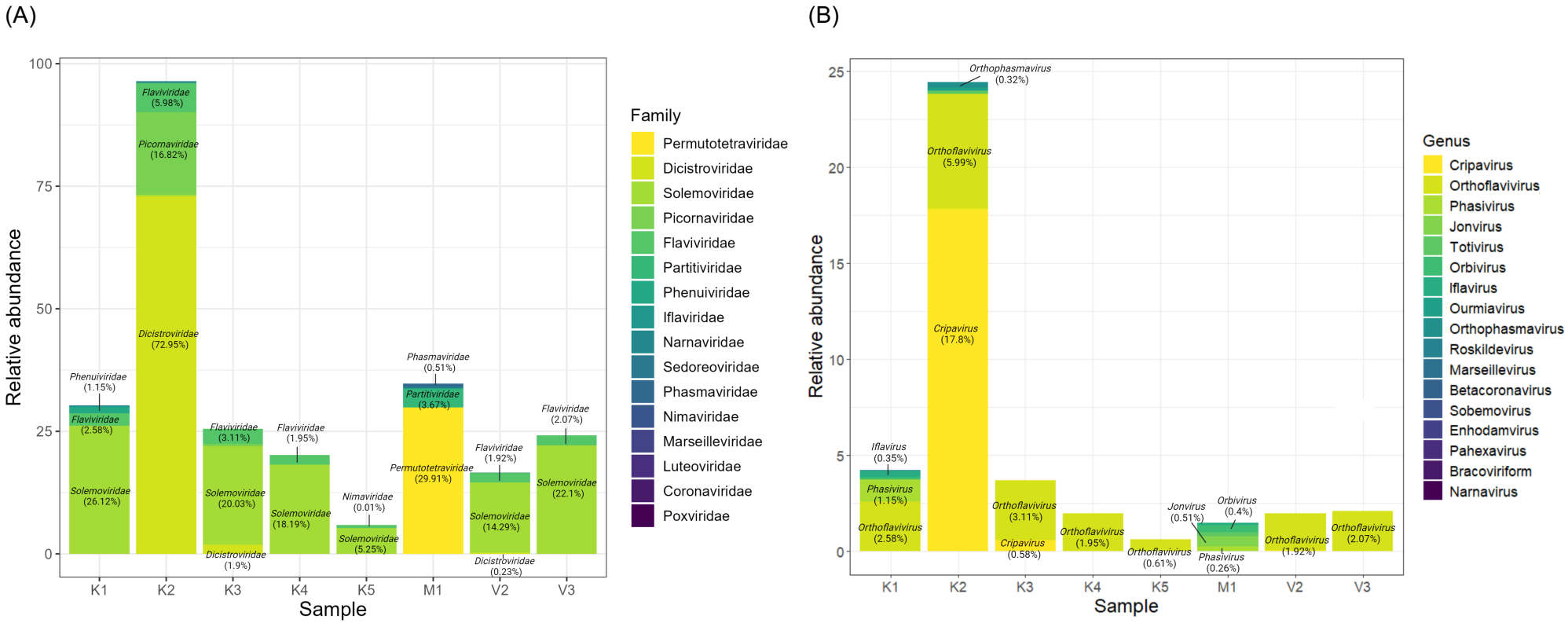

Figure S4. Viral families and genera in field mosquito pools (before filtering out those with <10 RPM or evidence of index-hopping). **A)** Top five families in each field mosquito pool; the top three families with relative abundance >0.1% in each pool are labeled. **B)** Top five genera in field mosquito pools; the top three genus with relative abundance >0.1% in each pool are labeled. Per International Committee on Taxonomy of Viruses recommendations, relative abundance of *Orthoflavivirus* comprises both *Orthoflavivirus* and *Flavivirus* identified by KrakenUniq.

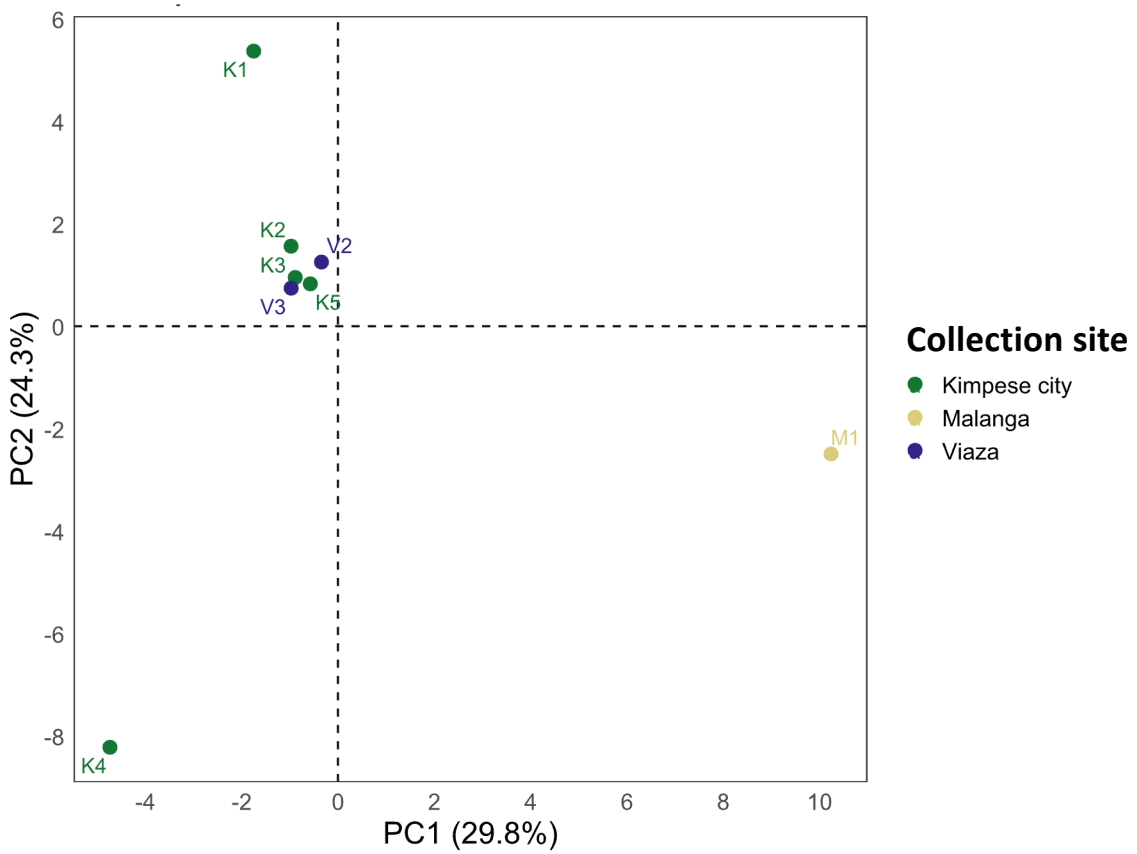

Figure S5. Principal component analysis (PCA) annotated by collection site using a data matrix containing relative abundance of viral genera (before applying the 10 RPM threshold and index-hopping filter).

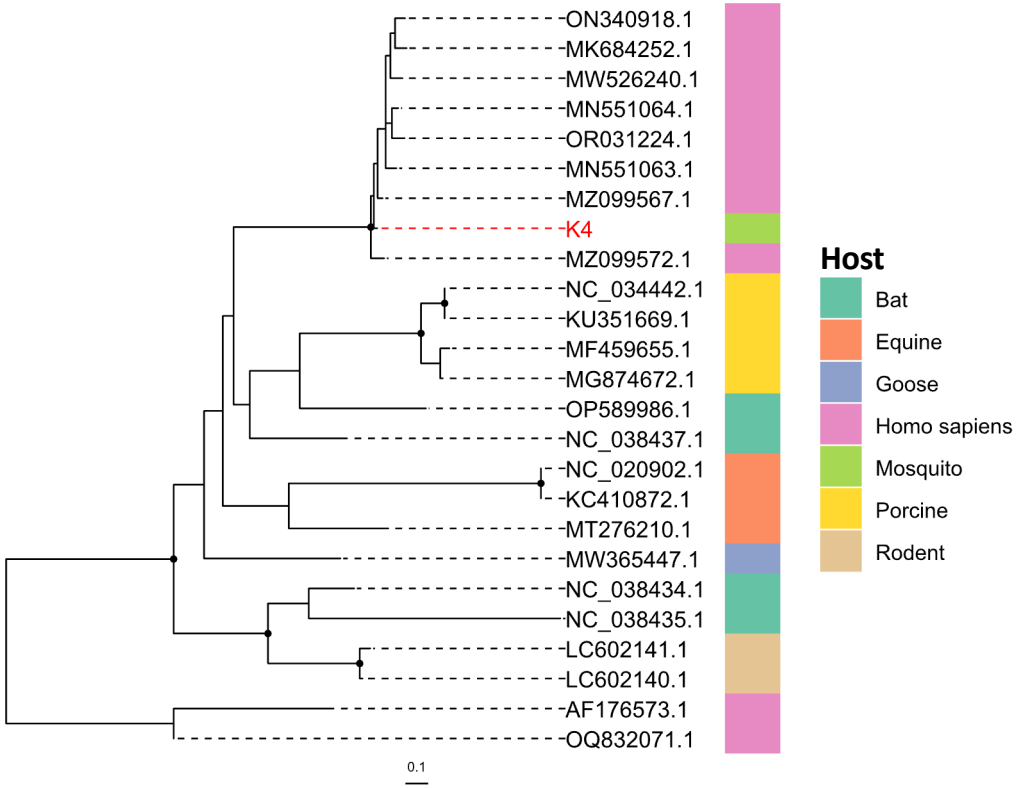

Figure S6. Phylogenetic analysis of pegivirus reads from a DRC field mosquito pool (red) compared to the polyprotein gene region of published sequences (black), constructed using RAxML-NG with the HKY+F+G4 model and hepatitis C virus sequences (AF176573.1 and OQ832071.1) as outgroups. Nodes with >70% bootstrap support across 1,000 replicates are annotated by a black circle.

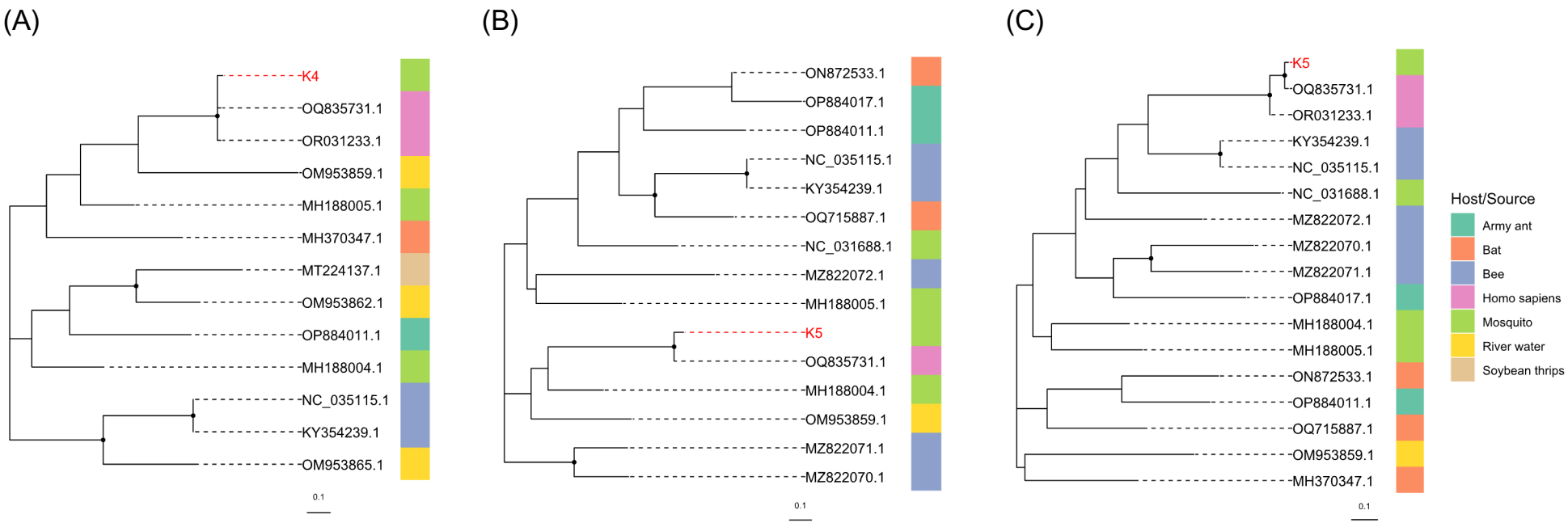

Figure S7. Phylogenetic analysis of human blood-associated dicistrovirus reads in DRC field mosquito pools (red) compared to published sequences (black), constructed using RAxML-NG with the HKY+F+I, HKY+F, and TPM3+F+R2 models, respectively. Analysis of reads from pools **A)** K4 and **B)** K5 mapping to the open reading frame 2 (ORF2) region, and **C)** from K5 mapping to the open reading frame 1 (ORF1) region. Nodes with >70% bootstrap support across 1,000 replicates are annotated by a black circle.